

# Fire resistance evaluation of fiber-reinforced cement composites using cellulose nanocrystals

Hyung-Joo Lee<sup>1</sup>, Seung-Ki Kim<sup>1</sup>, Heon-Seok Lee<sup>1</sup>, Yong-Hak Kang<sup>2</sup>,  
Woosuk Kim\*<sup>1</sup> and Thomas H.-K. Kang<sup>3</sup>

<sup>1</sup>Department of Architectural Engineering, Kumoh National Institute of Technology,  
61 Daehak-ro, Gumi, Gyeongsangbuk-do 39177, Republic of Korea

<sup>2</sup>Daegu & Gyeongbuk Branch, Korea Conformity Laboratories, Daegu 42994, Republic of Korea

<sup>3</sup>Department of Architecture & Architectural Engineering, Seoul National University, Seoul 08826, Republic of Korea

(Received April 18, 2019, Revised October 6, 2019, Accepted November 2, 2019)

**Abstract.** In this study, the effect of cellulose nanocrystals (CNCs) on the fire resistance properties of fiber-reinforced cement composites was investigated. The main variables were CNCs content (0.4, 0.8 and 1.2vol.% compared with cement), steel fiber ratio, and exposure temperature (100, 200, 400, 600 and 800°C). The fire resistance properties, i.e., residual compressive strength, flexural strength, and porosity, were evaluated in relation with the exposure temperature of the specimens. The CNCs suspensions were prepared to composited dispersion method of magnetic stirring and ultra-sonication. CNCs are effective for increasing the compressive strength at high temperatures but CNCs do not seem to have a significant effect on flexural reinforcement. Porosity test result showed CNCs reduce the non-hydration area inside the cement and promote hydration.

**Keywords:** Cellulose Nanocrystals (CNCs); fire resistance; porosity; residual strength; microstructure

## 1. Introduction

Recently, research on the development of various composites using the excellent physical properties of nanomaterials has been conducted. Polymer composite applications of these nanomaterials are already being used in the construction industry. However, the use of nanomaterials as construction materials is still in its infancy; hence, various nanomaterials are currently under development. The best-known nanomaterials applied to cement composites are carbon nanotubes (CNT). Although CNT have several vulnerabilities and economic problems, its use on cement composites has demonstrated significant improvement in the material's properties (Oh *et al.* 2018, Oh *et al.* 2017). Research conducted at home and abroad has identified that the addition of various nanomaterials to cement composites is effective for applications in the construction field (Norhasri *et al.* 2017). One of these nanomaterials is cellulose nanocrystals (CNCs), as described in this study. CNCs is kind of nanocellulose, which has a classified extraction method. CNCs are formed by chemical processes and cellulose nanofibers (CNFs) are formed by mechanical processes (Sofla *et al.* 2016). Although the research on cement composites using nanocellulose is currently in its early stages, many previous studies have shown that the performance of cement composites can be improved. Mazlan *et al.* (2016) studied that CNCs improved C-S-H (Calcium-Silicate-Hydrate) gel

formation and the strength of cement composites by up to 45% (Mazlan *et al.* 2016). Cao *et al.* (2015) identified the mechanism by which hydration is improved the strength of a part.

The purpose of this study is to evaluate the fire resistance of various CNCs cement composites by analyzing their physical and chemical properties. To this end, residual compressive strength, flexural strength, and porosity experiments were conducted through Mercury Intrusion Porosimetry (MIP).

## 2. Review of existing research

Previous studies on cement composites using CNCs have been conducted mainly on the evaluation of physical properties. Their related contents are listed in Table 1.

Various studies on the properties of cement composites using CNCs have been conducted at home and abroad. However, most researches have studied the strength properties and formation mechanisms of CNCs and cement composites, and no study on fire resistance has been found.

Due to the lack of studies on fire resistance regarding the cement composites containing CNCs, the studies on fire resistance evaluation of cement composites have been compiled. These studies are listed in Table 2.

Various studies on fire resistance evaluation of cement mortar have been actively conducted at home and abroad. The evaluation methods include residual strength, SEM, XRD, MIP and TG analyses. In this study, the residual strength and MIP analysis were selected for the fire resistance evaluation of cement composites containing CNCs.

---

\*Corresponding author, Professor  
E-mail: kimw@kumoh.ac.kr

Table 1 Review of existing literature on CNCs cement composite

Author	Contents
Cao <i>et al.</i> (2016)	This research studied the influence of raw and sonicated cellulose nanocrystals (CNCs) on the microstructure of cement paste. As a result of water desorption tests, the porosity of the plain cement paste was 16%. Conversely, porosity of cement paste containing raw and ultrasonic treated CNCs decreased to 14.8% and 14.4%, respectively. The reduction in porosity was the result of an increase in hydration. In addition, the use of CNC ultrasonic treatment was found to avoid aggregates that could lead to pore and air trapping.
Fu <i>et al.</i> (2017)	In this study, a total of 9 CNCs samples were used in Type I / II and Type V cement. The samples were analyzed by isothermal calorimetry (IC), thermogravimetric analysis (TGA), and ball-on-three-ball (B3B) flexural strength test. The performance of the CNCs cement composite was evaluated. IC and TGA showed that CNCs increased hydration in all specimens, and increased heat release in Type V cement, compared to Type I / II cement. The B3B flexural test showed a 20% increase in flexural strength in all cements.
Cao <i>et al.</i> (2015)	This study evaluated the effect of CNCs in cement paste through flexural strength, isothermal calorimetry (IC), thermogravimetric analysis (TGA), and degree of hydration (DOH). The increase of DOH was observed when CNCs were used. Two mechanisms of increased hydration were suggested when using CNCs. The results indicate that short circuit diffusion was more dominant than steric stabilization.
Mazlan <i>et al.</i> (2016)	Flowability, compressive strength, and SEM analyses were conducted to evaluate the effect of CNCs in cement mortar. Cement mortar strength improved 40~45% when CNCs were used. The existing shapes of CNCs looked similar to nano-needle fiber. It assisted the mortar structure to sustain more load by performing as bridging agents, thus holding the mortar matrix together.

Table 2 Review of existing literature about fire resistance on cement composites

Author	Contents
Kim <i>et al.</i> (2014)	This study conducted investigation on fire resistance and explosive properties of high strength concrete through residual strength, elastic modulus, and SEM analyses. The residual compressive strength of high-strength concrete was 20~40% at 700 °C in preliminary studies. In this study, a range of 38% was proven again. The experiment results indicated similar results to preliminary studies regarding fire resistance.
Lee <i>et al.</i> (2013)	The performance of the cement composite containing polypropylene fiber was evaluated. Flowability, density, compressive strength, and tension strength experiments were conducted. A mix of polypropylene beads and an antifoamer showed high performance regarding strength and ductility.
Kim <i>et al.</i> (2008)	The porosity and pore size distribution of cement paste and concrete were measured and analyzed by MIP analysis. As the water-cement ratio increased, the porosity increased. Conversely, the porosity decreased with hydration. In plain concrete, the porosity decreased as the amount of binder increased.
Kang <i>et al.</i> (2015)	The microstructure and pore structure of cement mortar exposed to high temperature were investigated. MIP, TG, and under-water weighing analyses were conducted to investigate the relationship between decomposition of hydration and changes in pore structure.
Mendes <i>et al.</i> (2012)	The difference between the dehydration and rehydration processes of cement paste and concrete exposed to high temperature was analyzed. Moisture adsorption tests and pore tests were conducted.
Çavdar Ahmet (2012)	The effect of fiber on the mechanical properties of cement mortar at high temperature was evaluated. Four fibers, polypropylene (PP), carbon (CF), glass (GF), and polyvinyl alcohol (PVA), and their fiber ratios were the main parameters.
Seleem <i>et al.</i> (2011)	The effect of pozzolana on the fire resistance of concrete was analyzed. Four types of pozzolana were used as the concrete mixture. The residual compressive strength and XRD analyses were conducted to evaluate the effect of the pozzolana.
Chen and Wu (2013)	The changes of pore structure of cement mortar relative to water-cement ratio and hydration period were analyzed and the experimental results were compared and examined with the existing models.
Tufail <i>et al.</i> (2017)	This study evaluated the mechanical properties of limestone, quartzite and granite concrete on high temperature. The compressive and split tensile strength, and modulus of elasticity decreased with increasing temperature, while the ultimate strain in compression increased.
Han <i>et al.</i> (2008)	This study investigated the spalling properties of high strength concrete designed with various types of mineral admixture and diverse content ratios of polypropylene fiber.
Tomasz <i>et al.</i> (2018)	This study focus the investigation of mechanical properties of self-compacting concrete with steel fiber after being exposed to fire. Flexural strength, equivalent flexural strength and micro-cracking after fire tests were tested.
Shaikh and Taweel (2015)	This study investigated the effects of temperatures of 400 °C and 800 °C on the residual compressive strength and failure behavior of fiber reinforced and unreinforced concrete. Steel fibers and basalt fiber are used in this study. The residual compressive strength of steel fiber reinforced concrete is higher than unreinforced concrete. But basalt fiber reinforced concrete showed lower strength than unreinforced concrete.

### 3. Experiments

#### 3.1 Preparation of CNCs suspension

The CNCs were dispersed prior to their mixing with the cement. Two methods were used for the dispersion of CNCs: magnetic stir and ultrasonication. The first dispersion process consisted of using a magnetic stirrer operating at 1300 RPM for 30 minutes, and the second one consisted in applying 2000 J of energy per 1 g of the CNCs



Fig. 1 Magnetic stirrer



Fig. 2 Ultrasonication

Table 3 Mix proportion

	W	C	FA	S	CNC (C-vol.%)	SP (C- wt.%)	Fiber (vol.%)
C04					0.4	0.75	
C08	0.3	0.8	0.2	0.37	0.8	1.25	1
C12					1.2	2.25	

C-vol.%: Volume fraction for cement, C-wt.%: Weight fraction for cement

through an ultrasonic dispersing machine. The magnetic stirrer and the ultrasonic dispersing machine used in the experiments are shown in Figs. 1 and 2, respectively. The CNCs suspension prepared by this method was used in various cement composite mixes.

### 3.2 Cement composite mix

The mixing ratios of the cement composites used in the experiment are listed in Table 3 below, with reference to the mixture of ECC (Engineered Cementitious Composite).

CNCs were mixed with cement in volume ratios of 0.4, 0.8, and 1.2%. When the CNCs were added, the viscosity of the compounding water increased and the flowability decreased. Therefore, the amount of the high performance water reducing agent was increased relative to the amount of CNCs. Steel fiber was used as the mixed fiber, and the mixing ratio was fixed to 1% of the total volume.

The mixing procedure was conducted as follows: The CNCs suspension was added in three times during mixing. This is to ensure that the mixed materials in the dry mixing state are evenly mixed to prevent material separation. In addition, in order to reduce the fiber ball phenomenon generated when the fiber is added, the compounding was carried out by adding a predetermined amount of fibers and dividing the CNCs suspension. Two cubic specimens of 50×50×50 mm were produced for the compression strength tests and two specimens of 40×40×160 mm were produced for the bending strength tests. After the mixing process, the specimens were placed in a curing room for 24 hours at 20°C. Thereafter, the cured product was demolded and subjected to high temperature steam curing for 48 hours. Test method was conducted referring to KS L ISO 679, KS L 5105. As shown in the regulations, the loading speed was tested according to the compressive strength of 2,400 N/s±200 N/s and the flexural strength of 50 N/s±10 N/s.



Fig. 3 Electric furnace



Fig. 4 Fire resistance test



Fig. 5 Compressive strength test set-up



Fig. 6 Flexural strength test set-up

### 3.3 Fire resistance experiment

Fire resistance experiments were conducted to determine the fire resistance performance of the cement composites containing CNCs.

In order to examine the material properties according to at low and high temperatures of the fabricated specimens, the specimens were heated to 20 (room temperature), 100, 200, 400, 600, and 800°C. The temperature increase rate was set at 2°C/min. After reaching the target temperature referring to KS F 2257-1, heating was finished after maintaining for 2 hours to satisfy the general fire resistance performance time. After heating, the electric furnace was

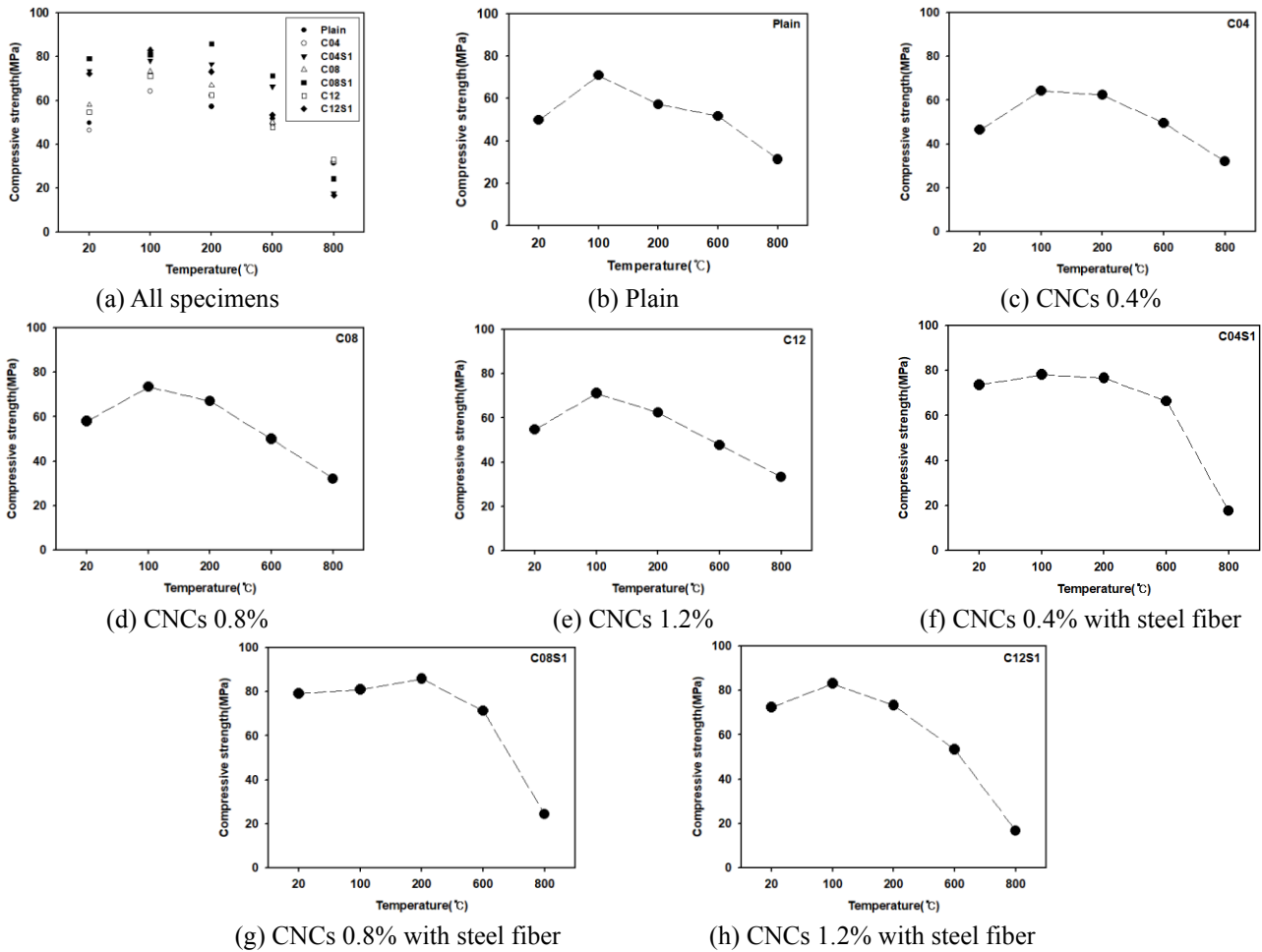


Fig. 7 Maximum of residual compressive strength relative to temperature

Table 4 Maximum strength of compression test (Unit: MPa)

Temp. (°C)	Plain	C04	C04S1	C08	C08S1	C12	C12S1
20	49.8	46.5	73.6	58.0	79.1	54.8	72.3
100	70.9	64.3	78.1	73.3	80.9	71.1	83.0
200	57.3	62.3	76.6	67.0	85.8	62.4	73.2
600	51.8	49.5	66.4	50.0	71.2	47.8	53.4
800	31.3	32.0	17.6	32.1	24.4	33.2	16.8

opened in order to cool it. After the heated specimen was sufficiently cool, the residual compressive strength and residual bending strength were measured. Figs. 3 to 6 below show the fire resistance and experimental view used in the experiment.

### 3.4 Porosity analysis

After the fire test, the porosity of the specimens was evaluated. MIP analysis was performed at a maximum pressure of 30,000 psi, a contact angle of 130 degrees, and a surface tension of 485 dynes/cm.

## 4. Experiment results

### 4.1 Residual compressive strength

The residual compressive strength of the specimens subjected to the fire test was measured. The experimental results are shown in Fig. 7 and listed in Table 4. The residual compressive strengths were different relative to the ratios of fiber and CNCs. In case of the plain specimens, the strength improved 50% at 100°C, and 15% at 200°C compared with those at room temperature. The residual strength at 600°C was similar to that room temperature, and decreased sharply at 800°C. Comparing the results of C04, C08, and C12 without incorporation of fibers, the highest compressive strength was obtained when 0.8% CNCs were incorporated. These results were similar in terms of residual compressive strength. The strength changes with increasing temperature were all similar, except for 800°C. The C08 specimen showed the highest compressive strength. It can be seen that the incorporation of CNCs affects the compressive strength, but not the residual compressive strength.

Comparing the results of C04S1, C08S1, and C12S1 with steel fiber, the C08S1 showed the highest compressive strength at room temperature, and 0.8% of CNCs was the most suitable mixing ratio. In case of C04S1 and C12S1, the strength decreased after 200°C. In case of C08S1, the strength increased steadily up to 400°C and then decreased. Except for C08S1, all specimens showed similar compressive strength patterns.

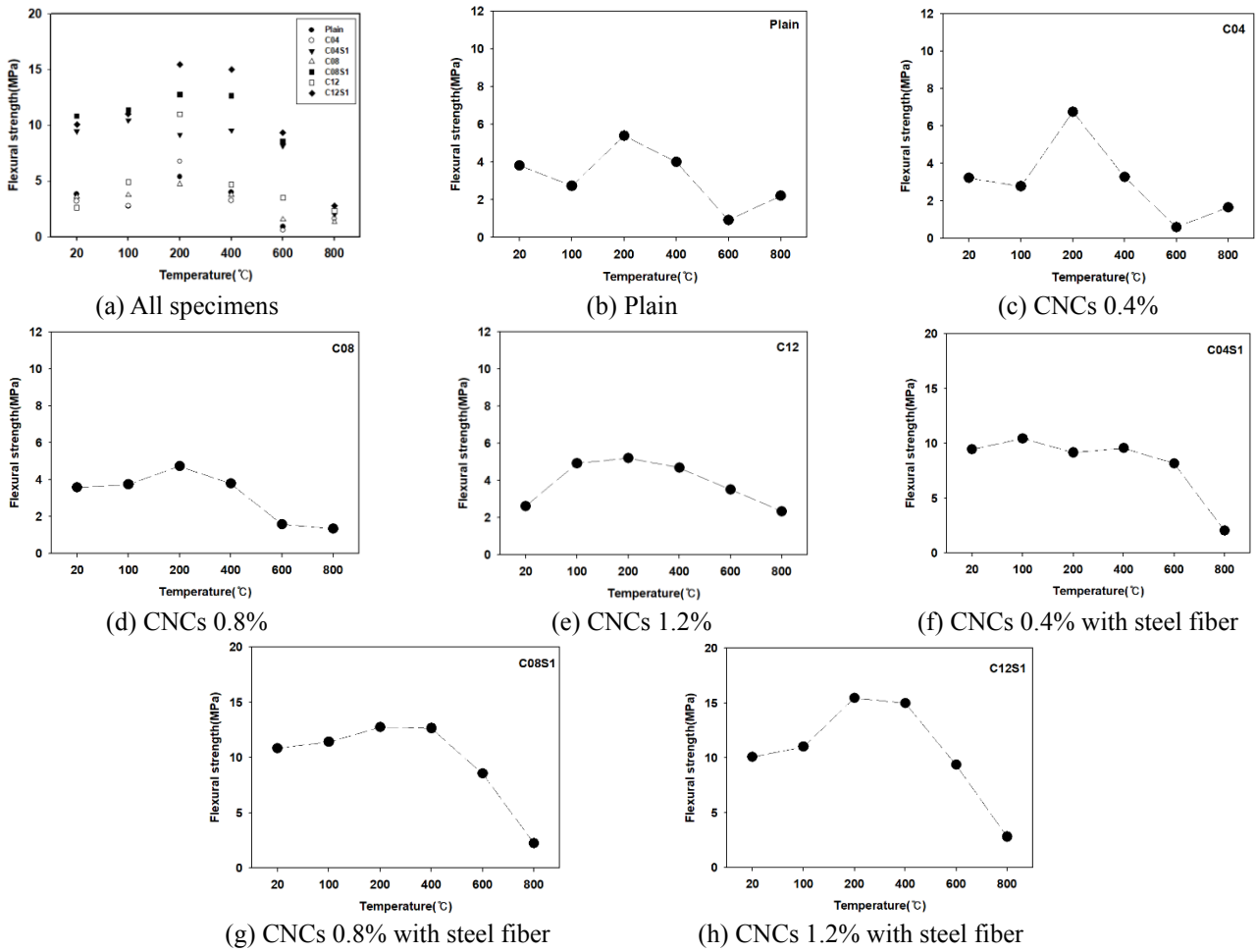


Fig. 8 Maximum residual flexural strength relative to temperature

The residual compressive strength test results show that the effect of steel fibers is greater than that of CNCs. The compressive strength at room temperature was 58%, 36%, and 32% higher than that of CNCs mixed with 0.4, 0.8, and 1.2%, respectively. The lower the mixing ratio of CNCs, the stronger the strength enhancement was.

4.2 Residual flexural strength and flexural toughness

The residual bending strength test was carried out after the fire test. The experimental results are shown in Figs. 8 and 9, and listed in Table 5. In the case of the plain specimen, it showed 2.73 MPa at 100°C, which is slightly lower than 3.82 MPa at room temperature. However, it increased to 5.4 MPa at 200°C, which is similar to the strength at room temperature, and then decreased when increasing the temperature to 600°C. The strength showed a rapid decrease due to the decomposition of the internal compound after 600°C. Comparing the results of C04, C08, and C12, C08 showed the highest bending strength with 3.58 MPa at room temperature. Bending strength of C04 decreased slightly but C08 and C12 increased compared to room temperature at 100°C. After 600°C, bending strength of the C04, C08, and C12 specimens decreased drastically.

C04S1 showed a slight increase and decrease in temperature after a slight increase in strength at 100°C and

Table 5 Maximum strength of flexural test (Unit: MPa)

Temp. (°C)	Plain	C04	C04S1	C08	C08S1	C12	C12S1
20	3.82	3.22	9.47	3.58	10.85	2.62	10.08
100	2.73	2.78	10.44	3.74	11.41	4.92	11.02
200	5.40	6.77	9.17	4.73	12.76	5.21	15.47
400	4.01	3.27	9.57	3.78	12.66	4.69	15.00
600	0.93	0.60	8.18	1.58	8.56	3.52	9.38
800	2.22	1.66	2.05	1.34	2.26	2.34	2.81

a sharp decrease in strength at 800°C. C08S1 and C12S1 exhibited higher flexural strength than that at room temperature up to 400°C, but decreased to a lower strength after 600°C and decreased rapidly at 800°C. As the mixing ratio of CNCs increased, the strength increased at 200°C and 400°C.

Fig. 9 shows the load-displacement curves of the plain, C04, C08, and C12 specimens without fiber. These showed typical brittle failure in which rupture occurred with sudden strength reduction after maximum load. There was no trend of load-displacement at 800°C, except for the C12 specimens without steel fibers and the C04, C12 specimens with steel fibers. This result is due to the fact that the test specimen is destroyed while applying a load.

In the case of the plain specimen, the behavior of the load-displacement curve with temperature did not show any

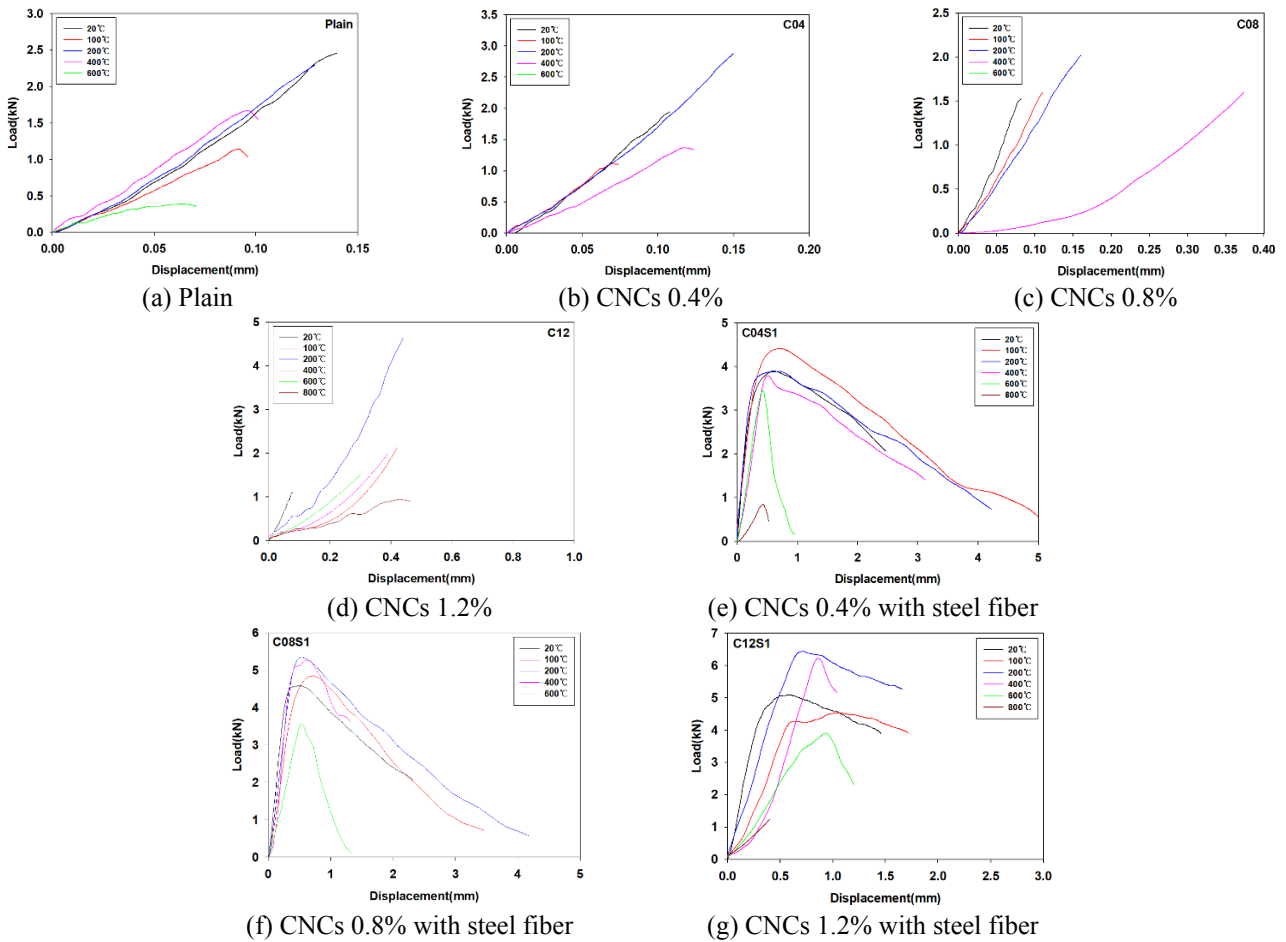


Fig. 9 Load-displacement curve of flexural strength specimens

significant change and the slope of the curve decreased at 600°C. In the case of C04, the slope of the load - displacement curve changed above 400°C. In C08, the slope gradually decreased as the temperature increased. C12 showed a large change in slope with temperature, but no linear trend is observed. The specimens with steel fiber showed ductile behavior in which the load gradually increased with increasing displacement after maximum load at all temperatures except 800°C. In addition, in all three test specimens, the slope of the curve gradually decreased as the temperature increased.

The maximum loads of the plain, C04, C08, and C12 specimens with no ductility behavior were obtained by calculating the area of zero point to maximum load ( $A_P$ ). The C04S1, C08S1, and C12S1 specimens with ductility behavior were evaluated in terms of the flexural toughness index, which is calculated by the area of zero point of the maximum load ( $A_P$ ) divided by the area ( $A_{P,80}$ ). Thus, it can be seen that the load was reduced by 80% of the maximum load.

The results of the flexural toughness evaluation of the test specimens are shown in Figs. 10 and 11. As shown in Fig. 10, the flexural toughness of the specimens without fiber showed no significant difference, and C12 showed the highest value. The strength and fracture displacement of specimens incorporating steel fiber greatly increased, indicating that the flexural toughness was also increased

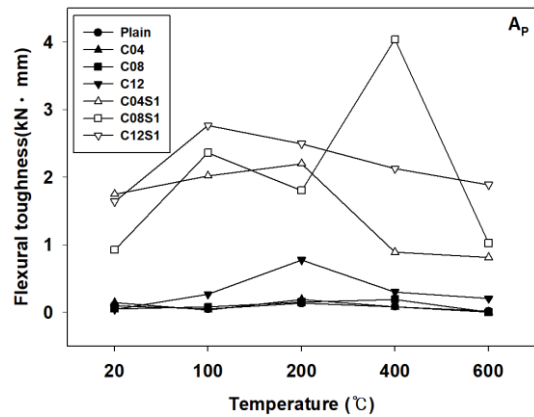


Fig. 10 Graph of flexural toughness ( $A_P$ )

when compared with the specimens not containing fibers. Up to 600°C, the trend of flexural toughness was similar on temperature, but the C08S1 showed a large difference only at 400°C.

The flexural toughness index of Fig. 11 shows that C04S1 slightly increased at 100°C and then decreased with the increasing temperature. However, it showed a rapid increase at 400°C, which is considered to be related to the decrease of the  $A_P$  value when the temperature changed from 200°C to 400°C. C08S1 exhibited a flexural toughness index value 1.5 times higher than that of other specimens at

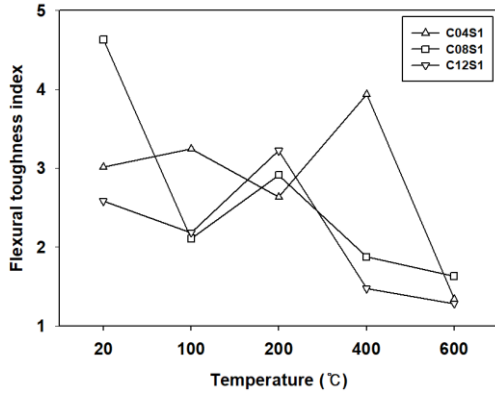
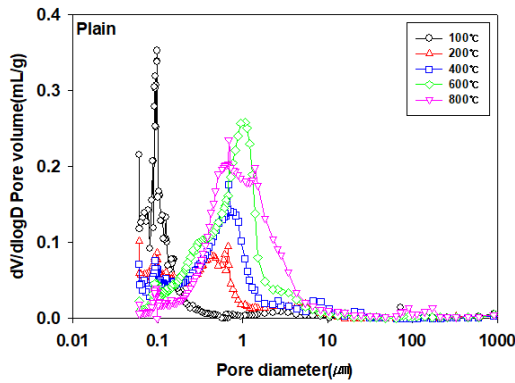
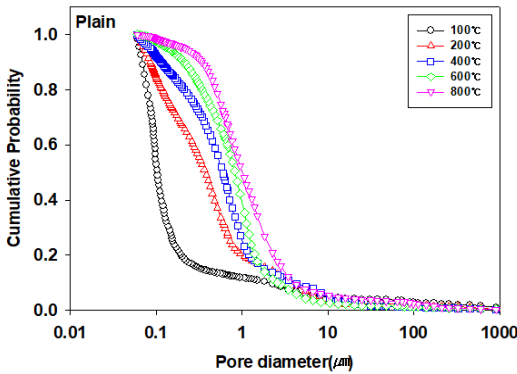


Fig. 11 Flexural toughness index



(a) Differential intruded volume-pore diameter curve



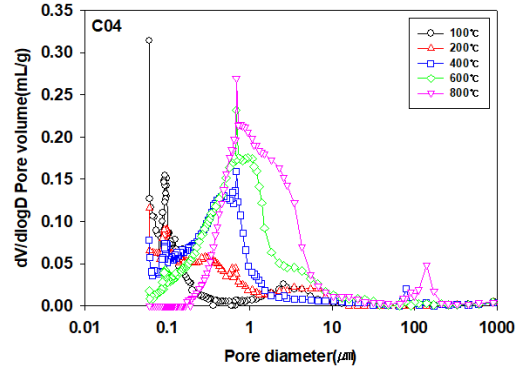
(b) Cumulative probability-pore diameter curve

Fig. 12 The result of MIP analysis on plain specimen

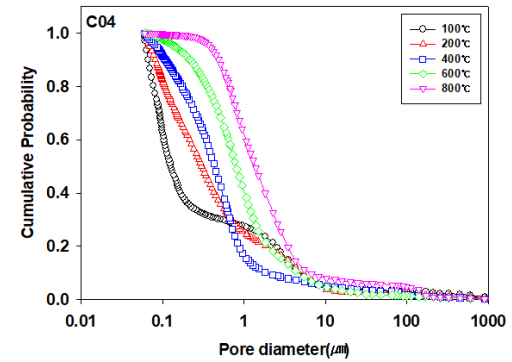
room temperature. However, the index decreased with the increasing temperature. The flexural toughness index of C12S1 increased slightly at 200°C, but then decreased. It is considered that the ductility was almost lost regardless of the mixing ratio of CNCs above temperatures of 600°C.

### 4.3 Porosity analysis

MIP analysis was carried out to analyze the microstructure of the cement composites subjected to the fire test. The experimental results are shown in Figs. 12 to 15 below. Fig. 12 shows the MIP results of the plain specimen. Fig. 12(a) shows the volume relative to the pore diameter, and Fig. 12(b) shows the integral value relative to the pore diameter. It can be seen that the pore diameter is



(a) Differential intruded volume-pore diameter curve



(b) Cumulative probability-pore diameter curve

Fig. 13 The result of MIP analysis on CNCs 0.4% specimen

concentrated at about 0.1 μm at 100°C, and the slope of the integral curve also increased sharply at approximately 0.1 μm. At 200°C, the pore diameter was widely distributed between 0.1 μm and 1 μm, and the pore diameter was increased compared to 100°C. It can be confirmed that the distribution of the voids was shifted to 1 μm at 400°C, rather than at 200°C. However, most of the pores were distributed at a value lower than 1 μm. Most of the pores were distributed at 1 μm at 600°C and the pores were distributed widely at about 1 μm at 800°C while increasing the deviation of the pores from 600°C. In Fig. 12(b), the curve shifted to the right as the exposure temperature increased, and the region where the slope rapidly increased also shifted to the right. As a result, the pore diameter increased as the exposure temperature increased.

The C04 specimen showed the highest peak between 0.06 and 0.1 μm at 100°C. At 200°C, the peak diameter was similar to 100°C, but the volume of diameters over 0.1 μm increased. At 400°C, the peak near 0.1 μm decreased and the peak at 1 μm rapidly increased. At 600°C, the peak at 1 μm slightly increased and the peak at 0.1 μm slightly decreased, but the overall pattern was similar to that at 400°C. At 800°C, the peak position was similar to 400°C, but the volume below 1 μm decreased and the volume above 1 μm increased.

The C08 specimen showed the highest peak at 0.1 μm, similar to the plain specimen at 100°C, and the peak was broadly distributed between 0.1 and 0.5 μm at 200°C. Thereafter, the peak shifted to about 1 μm at 400°C, and the peak of 0.1 μm decreased to less than 200°C. At 600°C, the peak of 1 μm increased, while at 400 °C the peak of 0.1 μm

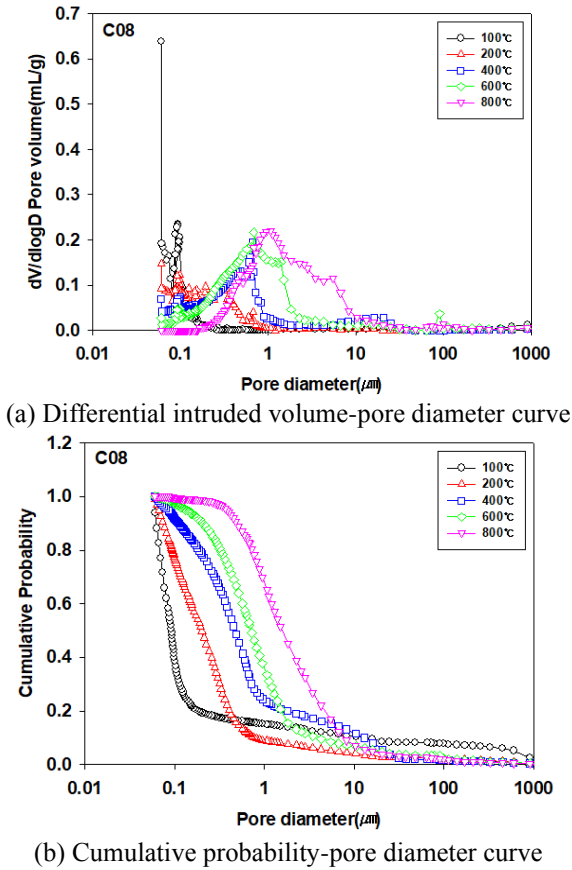


Fig. 14 The result of MIP analysis on CNCs 0.8% specimen

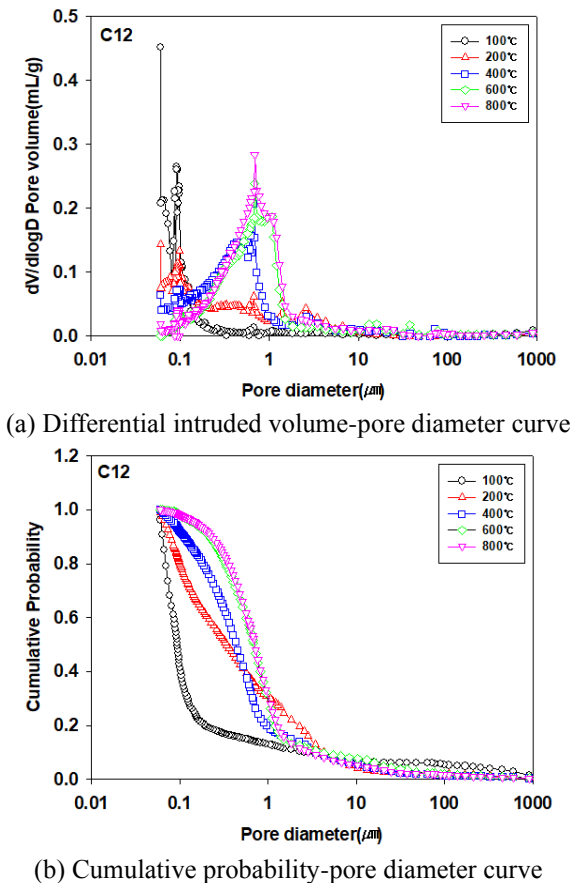


Fig. 15 The result of MIP analysis on CNCs 1.2% specimen

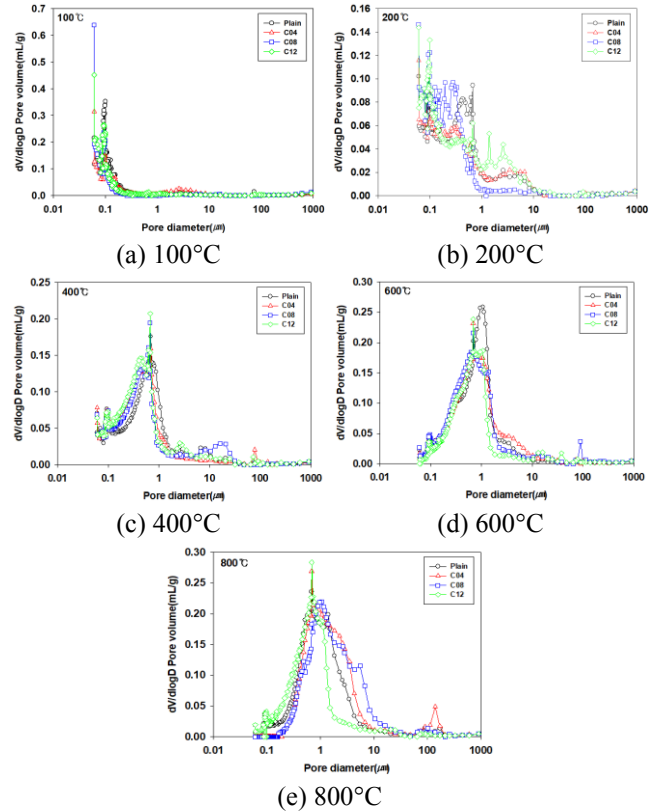


Fig. 16 The result of MIP analysis relative to exposed temperature

decreased and the peak of 1-1.5  $\mu\text{m}$  significantly increased. At 800°C, the curve shows a similar pattern to that at 600°C.

The C12 specimen showed a peak around 0.1  $\mu\text{m}$  at 100°C, and the highest peak at 0.06  $\mu\text{m}$ . This is similar to the results of the C04 and C08 test specimens. At 200°C, the 0.1  $\mu\text{m}$  peak slightly decreased and the peak value was broadly distributed in the range of 0.1 to 1  $\mu\text{m}$  at about 0.05 mL/g. At 400°C, the peak around 1  $\mu\text{m}$  greatly increased. At 600°C, the 1  $\mu\text{m}$  peak slightly increased. Overall, the pore shapes and diameters at 400°C were increased. At 800°C, the peak position and graph shape did not show any significant difference from those at 600°C. The average diameter was up to about 20% higher at 800°C than in the other specimens.

As a result of MIP analysis, there was no significant difference relative to the mixing ratio of CNCs. However, it can be seen that the pore diameters of the CNCs-incorporated specimens were slightly smaller than those of the plain specimen. The same peak was observed at 0.1  $\mu\text{m}$  at 100°C, but a higher peak was observed at about 0.06  $\mu\text{m}$  when CNCs were mixed. At 200°C, the overall curve shape was located to the left of the plain one, indicating that the pore diameter was relatively smaller. The shape and peak of the graph were similar in all the graphs from 400 to 800°C, but they were shifted to the left of the plain one. Through this, it was confirmed that the incorporation of CNCs can reduce the internal porosity of the cementitious composite exposed to high temperatures.

The results of MIP analyses relative to temperature are

shown in Fig. 16 below. The graph shapes of the plain and CNCs were similar. The CNCs-incorporated specimens at 100°C showed a peak at 0.06  $\mu\text{m}$ , but the plain specimen showed no significant difference except for a peak at 0.06  $\mu\text{m}$ . From 200°C onward, the CNCs-incorporated specimens are located on the left of the plot, which means that the pore diameter is relatively small.

## 5. Conclusions

The refractory performance and the microstructure analysis of the CNCs-incorporated cement composites were carried out. The experimental results are summarized as follows.

- CNCs were effective for increasing the compressive strength at room temperature, but did not affect the residual compressive strength. The C08 and C12 specimens showed higher compressive strength at room temperature than the plain, which was similar in residual compressive strength. The effect of mixing the cement composite with steel fiber was better than that of mixing it with CNCs.
- CNCs do not seem to have a significant effect on flexural reinforcement. The bending strength at room temperature was relatively reduced or similar depending on the mixing ratio of CNCs, but the aspect relative to the exposure temperature was different. However, the plain specimen, as well as the CNCs mixed specimens, exhibited similar or higher strength from room temperature up to 400°C, but the decreasing pattern after 600°C was the same. Also, deviation of flexural strength value was not greater than the compressive strength, except that the specimens were reinforced with steel fiber at each temperature. This result seems to be due to the brittle fracture pattern. In the future, the internal structure at high temperature should be analyzed by conducting precise analysis such as SEM and XRF.
- The flexural toughness through CNCs incorporation was evaluated. The plain specimen, as well as the CNCs mixed specimens, showed brittle fracture behavior at maximum load. It was considered that it is difficult to impart ductility to the cement composites only by the incorporation of CNCs, and it was confirmed that the reinforcing performance was improved when it was used together with steel fiber. The flexural toughness index gradually decreased with the increasing temperature, which means that toughness decreases gradually.
- Microstructure analysis showed that the pore diameters of the CNCs were smaller than those of the plain specimens, regardless of the exposure temperature. This result is related to the characteristics of CNCs, which reduce the non-hydration area inside the cement and promote hydration, as reported in the existing studies. However, due to the incorporation of CNCs, the pore size was reduced but it did not affect the strength increase at high temperatures.
- The strength improvement mechanism of CNCs promotes hydration in un-hydrated areas, thereby increasing the amount of hydration produced. The

increased hydration product is decomposed at a constant temperature. Decomposed hydration product is thought to show the appearance of voids and the resulting strength value decreases. Therefore, further research is needed to compare the amount of hydration products through Thermogravimetric analysis (TGA).

## Acknowledgements

The authors thank the Infrastructure and Transportation Technology Promotion Research Program funded by the Ministry of Land, Infrastructure and Transport of the Korean government, for all funding of this work under the grant [code# 18CTAP-C133534-02].

## Competing interests

The authors declare that they have no competing interests.

## Availability of data and materials

Not applicable.

## References

- Cao, Y., Zavaterra, P., Youngblood, P., Moon, R. and Weiss, J. (2015), "The influence of cellulose nano crystal additions on the performance of cement paste", *Cement Concrete Compos.*, **56**, 73-83.
- Cao, Y., Zavaterra, P., Youngblood, P., Moon, R. and Weiss, J. (2016), "The relationship between cellulose nanocrystal dispersion and strength", *Constr. Build. Mater.*, **119**, 71-79.
- Çavdar, A. (2012), "A study on the effects of high temperature on mechanical properties of fiber reinforced cementitious composites", *Compos. Part B*, **43**, 2452-2463.
- Chen, X. and Wu, S. (2013), "Influence of water-to-cement ratio and curing period on pore structure of cement mortar", *Constr. Build. Mater.*, **38**, 804-812.
- Fu, T., Montes, F., Suraneni, P., Youngblood, J. and Weiss, J. (2017), "The influence of cellulose nanocrystals on the hydration and flexural strength of Portland cement paste", *Polym.*, **9**(9), 424.
- Han, C.G., Han, M.C. and Heo, Y.S. (2008), "Spalling properties of high strength concrete mixed with various mineral admixtures subjected to fire", *Int. J. Concrete Struct. Mater.*, **2**(1), 41-48.
- Kang, S.M., Na, S.H., Kim, K.N. and Song, M.S. (2015), "Pore structure changes in hardened cement paste exposed to elevated temperature", *J. Korea Ceram. Soc.*, **52**(1), 48-55.
- Kim, T.S., Jung, S.H., Chae, S.T., Lee, B.C., Woo, Y.J. and Song, H.W. (2008), "An experimental study on the microstructure characteristics of cementitious composites by MIP", *Proc. Korea Concrete Inst.*, **20**(1), 533-536.
- Kim, W.S., Kang, T.H.-K. and Kim, W.J. (2014), "State-of-the-art research and experimental assessment on fire-resistance properties of high strength concrete", *J. Korea Inst. Struct. Mainten. Inspect.*, **18**(3), 28-39.
- Lee, B.Y., Bang, J.W. and Kim, Y.Y. (2013), "Enhancing the performance of polypropylene fiber reinforced cementitious

- composite produced with high volume fly ash”, *J. Korea Inst. Struct. Mainten. Inspect.*, **17**(3), 118-125.
- Mazlan, D., Din, M.F.M., Tokoro, C. and Ibrahim, I.S. (2016), “Cellulose nanocrystals addition effects on cement mortar matrix properties”, *Int. J. Adv. Mech. Civil Eng.*, **3**(3), 44-48.
- Mendes, A., Sanjayan, J.G., Gates, W.P. and Collins, F. (2012), “The influence of water absorption and porosity on the deterioration of cement paste and concrete exposed to elevated temperatures, as in a fire event”, *Cement Concrete Compos.*, **34**, 1067-1074.
- Norhasri, M.S.M, Hamidah, M.S. and Fadzil, A.M. (2017), “Applications of using nano material in concrete; A review”, *Constr. Build. Mater.*, **133**, 91-97.
- Oh, S.W., Jung, S.H., Chung, W.S. and Choi, Y.C. (2018), “Investigation of the effects of CNT dosages on the hydration and heating properties of cement composites with low water-to-binder ratio”, *J. Korea Inst. Struct. Mainten. Inspect.*, **22**(6), 182-188.
- Oh, S.W., Oh, K.S., Jung, S.H., Chung, W.S. and Yoo, S.W. (2017), “Effects of CNT additions on mechanical properties and microstructures of cement”, *J. Korea Inst. Struct. Mainten. Inspect.*, **21**(6), 162-168.
- Ponikiewski, T., Katzer, J., Kilijanek, A. and Kuzminska, E. (2018), “Mechanical behaviour of steel fibre reinforced SCC after being exposed to fire”, *Adv. Concrete Constr.*, **6**(6), 631-643.
- Seleem, H.E.D.H., Rashad, A.M. and Elsokary, T. (2011), “Effect of elevated temperature on physico-mechanical properties of blended cement concrete”, *Constr. Build. Mater.*, **25**, 1009-1017.
- Shaikh, F.U.A. and Taweel, M. (2015), “Compressive strength and failure behavior of fibre reinforced concrete at elevated temperatures”, *Adv. Concrete Constr.*, **3**(4), 283-293.
- Sofla, M.R.K., Brown, R.J., Tsuzuki, T. and Rainey, T.J. (2016), “A comparison of cellulose nanocrystals and cellulose nanofibres extracted from bagasse using acid and ball milling methods”, *Adv. Nat. Sci.: Nanosci. Nanotechnol.*, **7**, 1-9.
- Tufail, M., Shahzada, K., Gencturk, B. and Wei, J. (2017), “Effect of elevated temperature on mechanical properties of limestone, quartzite and granite concrete”, *Int. J. Concrete Struct. Mater.*, **11**(1), 17-28.